Research Article

BIOMEDICAL Journal of Scientific & Technical Research

ISSN: 2574 -1241

DOI: 10.26717/BJSTR.2022.41.006678

Monitoring BTEX Adsorption on to Organoclays in Aqueous Solution: Multi-isotherm and Kinetics Studies

Kelechi E Onwuka[1]*, Precious O Emole[1], Jude C Igwe[1] and Okechukwu C Atasie[2]

[1]*Department of Pure and Industrial Chemistry, Abia State University Uturu, Nigeria*

[2]*Department of Biochemistry, Abia State University Uturu, Nigeria*

***Corresponding author:** Kelechi E Onwuka, Department of Pure and Industrial Chemistry, Abia State University Uturu, P.M.B. 2000, Nigeria

ARTICLE INFO

Received: January 01, 2022

Published: February 16, 2022

Citation: Kelechi E Onwuka, Precious O Emole, Jude C Igwe, Okechukwu C Atasie. Monitoring BTEX Adsorption on to Organoclays in Aqueous Solution: Multi-isotherm and Kinetics Studies. Biomed J Sci & Tech Res 41(5)-2022. BJSTR. MS.ID.006678.

Keywords: Organoclay; BTEX; Adsorption Isotherm; Adsorption Kinetics; Montmorillonite

SUMMARY

The efficiency of hexadecyltrimethly ammonium and Triphenyl ammonium cation intercalated montmorillonite for sorption of benzene toluene, ethylbenzene and xylene (BTEX) in aqueous solution has been investigated. X-ray diffraction (XRD), Scanning electron microscopy (SEM) and Fourier Transform infrared spectroscopy (FTIR) were employed to characterize the adsorbents. From characterization, it is evident that the intercalation of montmorillonite's surface cations by those of HDTMA and TMPA cations resulted to a structural change in the surface of the adsorbents. Results from adsorption experiment confirmed 2 hours as optimum time for equilibrium sorption of BTEX by both modified and un-modified montmorillonite. The sorption mechanism of BTEX onto organoclay was assessed by subjecting sorption data to six isotherm models, namely: Langmuir, Freundlich, Dubnin Radushkevich, Temkin, Halsey And Harkins Jara isotherm models; and three kinetic models (Pseudo first order, Pseudo second order and intra-particle diffusion model), with results confirming Freundlich isotherm model and pseudo second order kinetic models as best fit to experimental data, thereby implying suitability of organaomontmorillonite for BTEX sorption.

Abbreviations: XRD: X-ray Diffraction; SEM: Scanning Electron Microscopy; FTIR: Fourier Transform Infrared Spectroscopy; VOC: Volatile Organic Compounds; BTEX: Benzene Toluene; Ethylbenzene and Xylene

Introduction

The vast amount of organic pollutants such as BTEX, PAHs, Phenols etc, present in the aquatic environment today is a matter of global concern which requires an urgent attention. BTEX is the acronym for the group of volatile organic compounds (VOCs) benzene, toluene, ethylbenzene and xylene. Anthropogenic sources of BTEX in ambient air largely include petrochemical fuel derivatives such as petrol or gasoline, automobile emissions, and the use of solvents and paints [1-6]. In urban areas, the combustion of gasoline and diesel fuels, especially for motor vehicles, constitutes the most important source of BTEX [6-10]. BTEX compounds are volatile and easily vaporize at temperatures above 200°C, and hence fugitive emissions from fuel storage facilities and transportation activities are also important sources of BTEX [9,11]. A number of studies have reported high ambient concentrations of BTEX during fuel tank filling [12-14], from oil and gas operations [14-16], and during solvent usage and spills from accidents [10,14].

It is known from the literature that these compounds have a negative impact on the environment since they contribute to the formation of ozone and other photochemical oxidants [17,18]. Moreover, BTEX are either known for being, or suspected to be, irritants, neurotoxins, allergens or carcinogens [19] and their exposure on a long term basis presents a serious threat to the human health [20,21]. Therefore, implementing effective strategies for pollution control is of paramount importance to limit human exposure and prevent environment degradation [18,22]. Many conventional methods can be employed to remove BTX from water and wastewater, including adsorption, aeration, biological oxidation and chemical oxidation [18]. Of these, adsorption processes involving porous solids are the most popular, and are widely utilized in engineering practice since they permit the recovery of these compounds [23]. Various mineral and organo-mineral sorbents have recently been regarded as alternative adsorbents which are potentially useful for the removal of BTX from water [24-40].

Clay is generally considered ineffective for sorption of hydrophobic organic compounds like BTEX and Polycyclic aromatic hydrocarbons (PAHs) due to its hydrophilic surface [33,40]. Montmorillonites (MMT) are commonly used clays owing to their high cation exchange capacity (CEC), swelling properties, and high surface areas but they are hydrophilic but can be modified for hydrophobic sorption by a simple organophilicization achieved by ion exchange reaction between clay surface ions and those of organic cations [33,40,41]. In attempt to design this new adsorbents to remove non-ionic organic contaminants from waste water, several researchers have replaced the inorganic exchange cations with quaternary amine cations [(CH3)2NHR]+, where R is a large alkyl hydrocarbon chain, yields organoclays with organophilic clay surfaces, by simple ion-exchange reaction [42,43]. It is generally accepted that adsorption of hydropholic long-chain quaternary ammonium cations onto clays occurs according to the ion-exchange mechanism [44,45].

The adsorption extent of such cations can approach double the cation-exchange capacity (CEC). Earlier workers reported that the lyophilic tails from cations of long-chain quaternary ammonium salts, previously retained on the clay, lead to the adsorption of organics such as benzene, toluene, phenol, and its chlorinated compounds and herbicides [43,45,46]. Therefore, the present study monitors BTEX Adsorption by HDTMA+ and TMPA+ Intercalated Montmorillonite clay. Effect of adsorption parameters such as contact time and initial adsorbate concentration, multiple adsorption isotherms and kinetic models were used to study the sorption mechanism.

Experimentals

Adsorbents

The montmorillonite (Mt) clay exploited in this research were collected from Ropp, Plateau State, situated at Longitude 80E and Latitude 90N, Northern Nigeria, and the clay was beneficiated according to our previous study [40]. The pure Mt was pre-modified by adopting the methods of Baskaralingam [47]. High-purity Mt was mixed with sufficient amount of 1M NaCl using a mechanical stirrer (6000 rpm for 24h) at room temperature of 250°C. The Na-Mt was then separated and washed four times with distilled water to remove any trace of chlorides, which was confirmed by the addition of 1M $AgNO_3$, resulting to the absence of a white or off-white precipitate. Wanders and Fourie's Procedure [48] was followed to impregnate the pre-modified Montmorillonite (Na-Mt). 21 g of Na-Mt each was separately added to 0.54 L of distilled water. The impregnated Na-Mt was prepared by separately adding the surfactants (HDTMA and TMPA) to their individual mass value equivalent to twice the clays' CEC. The mixtures were separately kept in suspension for 24 hours at 160 rpm and 25°C by using a temperature controlled orbital shaker. The impregnated Na-Mt was washed with distilled water and dried at 70°C for 24 hours, and were designated as Mt-HDTA and Mt-TMPA.

Adsorbent Characterization

The surface area of the adsorbents were determined by Sear's method [49] and cation exchange capacity (CEC) by the ammonium acetate procedure [50]. The morphological and X-ray diffraction properties of the adsorbents, as well as variation in functional groups were studied using scanning electron microscope (Leo 1455 VP), X-ray diffractometer (XRD-7000 Shimadzu) and Buck scientific M530 USA FTIR respectively. Detail of procedures employed in these characterization are available in our previously published work [40].

Adsorbate

Benzene (≥99%), toluene (99.5%), ethylbenzene (≥99%), and xylene (99.5%) were purchased from Sigma- Aldrich Chemical Company Switzerland. The BTEX standard solution (400 mg/L BTEX = 100 mg/L benzene + 100 mg/L toluene + 100 mg/L ethylbenzene + 100 mg/L xylene) was prepared in distilled water and kept at 40C. The stock solutions were further diluted by distilled water as working solutions.

Batch Adsorption Studies

Batch adsorption tests were carried out to assess the adsorption efficiency of the raw and surfactant modified clays (Mt,

Mt-HDTMA, Mt-TMPA). All adsorption experiments were carried out at room temperature (250°C) with 100 mL of BTEX solution into a 200 mL conical flask (with air tight cape) and shaken at 250 rpm for 24 h. After this, the suspensions were centrifuged (6000 rpm for 15 min) and the clear supernatant was then measured for BTEX by Gas chromatography (Agilent GC, 6890N), equipped with mass spectrometer detector. Blank samples (BTEX solution without the adsorbent) were also used to determine the value of BTEX volatilization. The BTEX loss due to the volatilization was estimated in percentage. The experimental data were corrected to account for volatilize BTEX. The adsorption capacities of Mt, Mt-HDTMA and Mt-TMPA for BTEX uptake were determined using:

$$q\_e = [c\_o - c\_e]\frac{v}{m} \quad (1)$$

where qe(mg/g) is the adsorption capacity of the adsorbent, Co(mg/L) is the initial concentration of the adsorbate, Ce (mg/L) is the equilibrium concentration of the adsorbate in the solution, m(g) is the mass of the adsorbent, and V(L) is the volume of the solution. The effect of contact time on the adsorption of BTEX by Mt, Mt-HDTMA, Mt-TMPA, was carried out, using 100 mL of a solution containing 0.5 g adsorbent and 50 mg/L BTEX solution (Benzene 10 mg/l, Toluene 10mg/l, Ethylbenzene 10 mg/l and Xylene 20 mg/l) at various contact times of 10, 20, 40, 60, 100 and 120 mins. In many industrial wastewaters the concentration of BTEX varies between 20 to 200 mg/L [51]. Hence, the effect of initial BTEX concentrations of 50, 100, 125, 150, and 200 mg/L on the adsorption efficiency was evaluated at optimum contact time and pH at 250°C.

Results and Disscussion

Surface Characterization

Table 1: Chemical composition of raw Montmorillonite.

Chemical composition (%)	Montmorillonite
SiO_2	60.6
Al_2O_3	20.03
Fe_2O_3	2.31
Na_2O	3.02
MgO	4.11
P_2O_5	0.05
K_2O	0.13
CaO	1.40
TiO_2	0.18
MnO	0.08
H_2O	8.62

Results of the experiments and analyses representing the chemical composition of raw adsorbents montmorillonite (Mt), and results for specific surface area and cation exchange capacity (CEC) of montmorillonite (Mt); HDTMA modified Montmorillonite (Mt-HDTMA); TMPA modified montmorillonite (Mt-TMPA) are represented in (Tables 1 & 2) respectively3.1.1. Surface

Area Determination and CEC Measurements

(Table 2). show the values for surface areas for montmorillonite (Mt), HDTMA modified montmorillonite (Mt-HDTMA), TMPA modified montmorillonite (Mt-TMPA). The modification of the adsorbents by Haxadecyltrimethylanonium bromide and Trimethylphenylamonium chloride led to reduction of surface areas for modified montmorrilonite from 39.1 m^2/g for Mt to 29.4 m^2/g and 24.87m^2/g for Mt HDTMA and Mt-TMPA respectively. These values for surface areas are in line with that obtained for raw and TTAB modified Montmorillonite clay by Nourmoradi et al. [33]. From the values obtained for CEC of montmorillonite (Mt), HDTMA modified montmorillonite (Mt-HDTMA), TMPA modified montmorillonite (Mt-TMPA), an increase in cation exchange capacity (CEC) from 78.51 meq/100g for Mt to 95.48meq/100g respectively was observed, corresponding to the values obtained by Nourmoradi et al [33]. Due to the favorable interlayer microenvironment created by the long chain alkyl ammonium ions for the partitioning of organic molecules, the size of the alkyl chain and the charge density of the clay layer are responsible for the arrangement of the intercalated cations corresponding to increase in the clay cation exchange capacity.

Table 2: Values for cation exchange capacity and specific surface area of montmorillonite (Mt); HDTMA modified Montmorillonite (Mt-HDTMA) and TMPA modified montmorillonite (Mt-TMPA).

Adsorbents	CEC (Meq/100g)	Surface area m^2/g
Mt	78.51	39.1
Mt-HDTMA	95.48	29.4
Mt-TMPA	84.51	24.87

FT-IR Spectroscopy

(Figure 1) represents FT-IR spectra of the adsorbents. FTIR spectroscopy has significantly contributed to the understanding of the structure, bonding, and reactivity of clay minerals [52]. FTIR spectra reveals the specific functional groups on montmorillonite and organoclay surface qualitatively based on the characteristics absorbed energy for each bonds in certain groups [53]. The examination of the IR spectra in the range 4000-400 cm^{-1} provides information on fundamental vibrational modes of the constituent

units of these materials [54]. OH, stretching and bending occur in the spectral region of 3750-3500 and 950-600 cm^{-1} respectively. Si-O and Al-O stretching modes are found in the 1200-700 cm^{-1} range while Si-O and Al-O bending modes dominate in the 600-400 cm^{-1} region [55]. IR spectra peak for unmodified montmorillonite clay indicates that the -OH bending band at 850.63cm^{-1} respectively were readily assigned to Al-OH.

The position and the shape of the -OH stretching band in the IR spectra of montmorillonite is basically influenced by the nature of the octahedral atoms to which the hydroxyl groups are contained [54,56]. The strong band located at 1157.6 cm^{-1} was the Si-O stretching vibrations, indicating that Si-O-Al and Si-O-Si bending vibrations respectively were typical of the tetrahedral Si-O. Bands at 3249.37cm^{-1}, 1612.6cm^{-1} are attributed to the OH stretching and bending vibrations of molecular water respectively. The quantity of adsorbed water in the clay is attributed to the deformation vibration of the H-O-H group (around 1631 cm^{-1}). Bands at around 1612.69cm^{-1} for montmorillonite (Mt) is a consequence of Si-O valence vibrations.

The addition of organic modifier-HDTMA and TMPA (Figure 1) increased the intensity at around 2898.3cm^{-1}, 2796.3cm^{-1} and 2840.53cm^{-1}, 3235.31cm^{-1} for HDTMA modified montmorillonite (Mt-HDTMA) and TMPA modified montmorillonite (Mt-TMPA) respectively. The absorption band at around 2898.3cm^{-1}, 2796.3cm^{-1} and 2840.53cm^{-1}, 3235.31cm^{-1} for HDTMA modified montmorillonite (Mt-HDTMA) and TMPA modified montmorillonite (Mt-TMPA) respectively corresponds to asymmetric and symmetric stretching methylene (CH2) bond [54,57]. Also, a bending vibration of the methylene groups can be seen at bands of 1613cm^{-1} for montmorillonite (Mt), verifying the intercalation of surfactant molecules between the silica and layers [54,58]. The change of the percentages of clay in the composite does not strongly affect the intensity of the remaining vibrational bands.

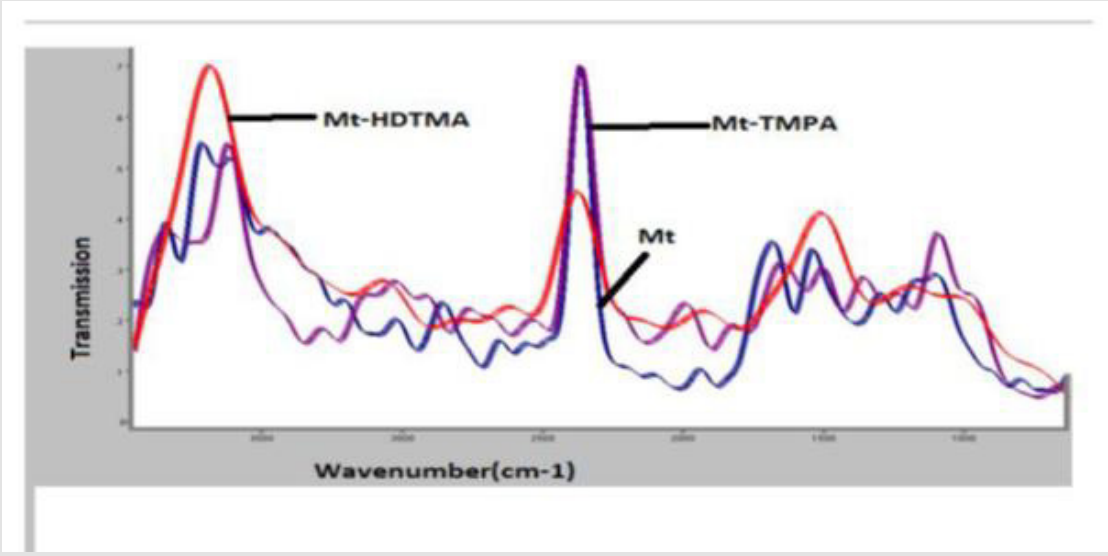

Figure 1: FT-IR Spectra of montmorillonite (Mt); HDTMA modified Montmorillonite (Mt-HDTMA) and TMPA modified montmorillonite (Mt-TMPA).

The AI-AI-OH stretching band typically occurs at 3620-3630 cm^{-1}, the AI-Mg-OH stretching band at 3695 cm^{-1} and the A1-Fe_3+-OH band at 3599 cm^{-1}. The frequency of maximum absorption thus indicates that the montmorillonite is Al-rich. The broadness of the band is due to the contribution of Mg and Fe in octahedral sheets and might also indicate, that the momtmorillonite structure is poorly ordered. The OH vibrations are better resolved in the bending frequencies as compared to the stretching frequencies. Other bands in the 1149-600 cm^{-1} region are the Si-O stretching bands at around 1149 cm^{-1} (in-plane) and 914 cm^{-1} (out-of-plane), the Al-O+Si-O out-of-plane vibration at 690.2 cm^{-1} for montmorillonite (Mt). Analysis of IR spectra confirmed that the organic modifiers-HDTMABr and TMPACl are strongly associated with montmorillonite when put in its interlayer space and this equally leads to the formation of a new composite, which, because of the different structure relative to the clays and the monomers, will have different properties [54,59,60]

Scanning Electron Microscopy (SEM)

The SEM images of montmorillonite (Mt), HDTMA modified montmorillonite (Mt-HDTMA), TMPA modified montmorillonite (Mt-TMPA) are presented in (Figure 2) (a-c). The surface structure of the adsorbent is changed by the modification with HDTMA and

TMPA. It can be seen that the surface textures of montmorillonite (Mt) are rough with irregular shapes. However, the surface morphologies of HDTMA modified montmorillonite (Mt-HDTMA) and TMPA modified montmorillonite (Mt-TMPA) are smoother than montmorillonite (Mt). This is due to the fact that the porous surfaces of montmorillonite is filled with surfactant. Similar results have been reported by Aivalioti et al [61]. Nourmoradi et al [33]. and Onwuka et al., [40]. The combined XRD patterns of montmorillonite (Mt), HDTMA modified montmorillonite (Mt-HDTMA), TMPA modified montmorillonite (Mt-TMPA) samples are shown in (Figure 3).

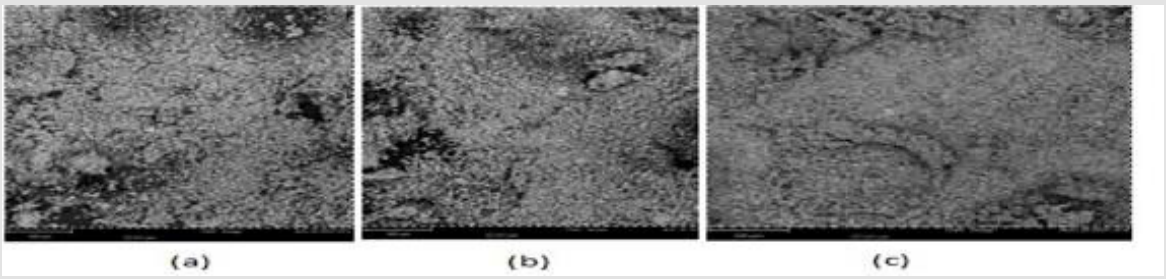

Figure 2: SEM images for
(a) Mt,
(b) Mt-HDTMA and
(c) Mt-TMPA.

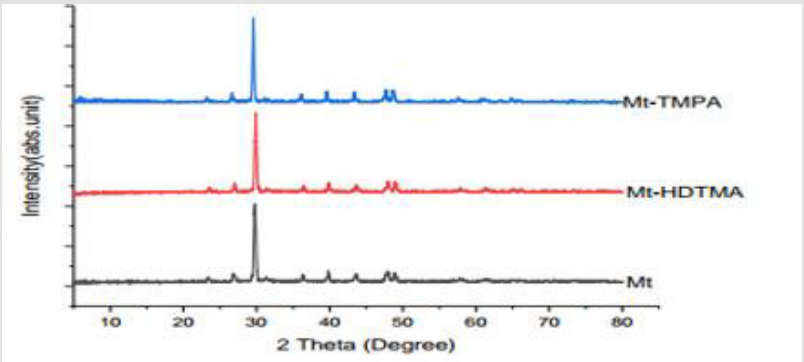

Figure 3: Combined XRD pattern for montmorillonite (Mt); HDTMA modified Montmorillonite (Mt-HDTMA) and TMPA modified montmorillonite (Mt-TMPA).

The XRD basal spacing ($d001$) of Mt, Mt-HDTMA, Mt-TMPA, Bt, Bt-HDTMA and Bt-TMPA were found to be 12.004Å, 16.780Å,15.834Å respectively. Moreover, increasing the reflection intensity from 2.52% for Mt to 100% for both Mt-HDTMA and Mt-TMPA respectively showed that the surfactant modification has led to structural changes in Mt. The interlamellar expansion in the modified adsorbent is attributed to the penetration of haxadecyltrimethylanonium cation and trimethylphenylamonium cation into the layers of Mt. The values of basal spacing obtained are in agreement with that reported in the literature [62]. The cation exchange reactions have been traditionally exploited as an effective method to replace inorganic ions with organic cationic surfactant molecules which intercalate into the clay gallery, resulting in expansion of the interlayer spacing thereby leading to an increase in the basal spacing [63-66].

The adsorption data for BTEX uptake by montmorillonite (Mt), HDTMA modified montmorillonite (Mt-HDTMA), TMPA modified montmorillonite (Mt-TMPA) are presented in (Figures 4-6) respectively. The adsorption capacity of BTEX using modified adsorbent has been rapidly increased at the beginning of contact time which could be due to the availability of more adsorption sites [33,40,66]. Then the adsorption capacity increases slowly up to about up to 120 mins. The adsorption capacities of Mt, Mt-HDTMA and Mt-TMPA at the first 60mins of the adsorption was determined to be 0.12 mg/g, 0.10 mg/g, 0.11 mg/g, 0.418 mg/g; 1.208 mg/g, 1.396 mg/g, 1.596 mg/g 3.768 mg/g; 1.066 mg/g, 1.412 mg/g, 1.426 mg/g, 3.478 mg/g for benzene, toluene, ethylbenzene, and xylene, respectively. But the corresponding adsorption capacity at the equilibrium time was estimated to be 0.168 mg/g, 0.144 mg/g, 0.352 mg/g, 0.438 mg/g; 1.228 mg/g, 1.462 mg/g, 2.132 mg/g, 4.504 mg/g; 1.724 mg/g, 1.506 mg/g, 2.584 mg/g, 4.618 mg/g.

DOI: 10.26717/BJSTR.2022.41.006678

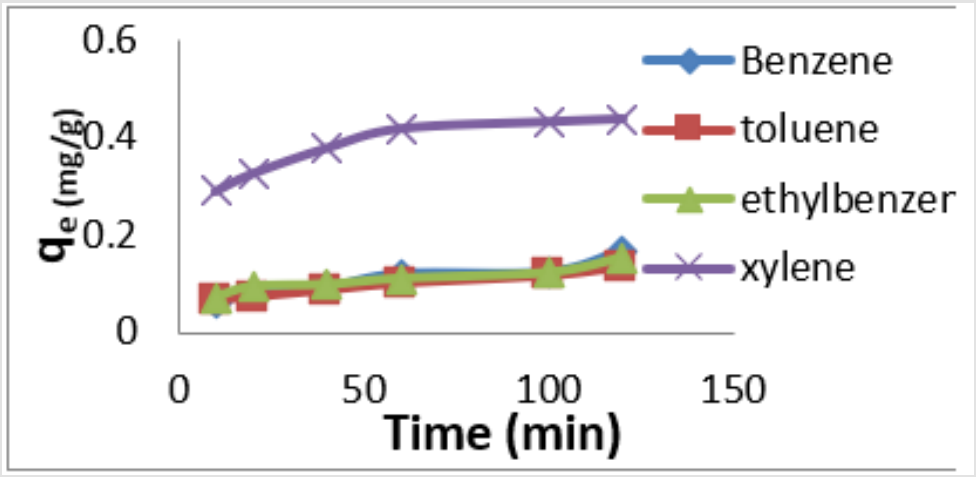

Figure 4: Effect of contact time on the adsorption of BTEX using Mt (BTEX solution = 50mg/L, initial pH= 7±0.5, contact time = 2hours, Mt = 0.5g).

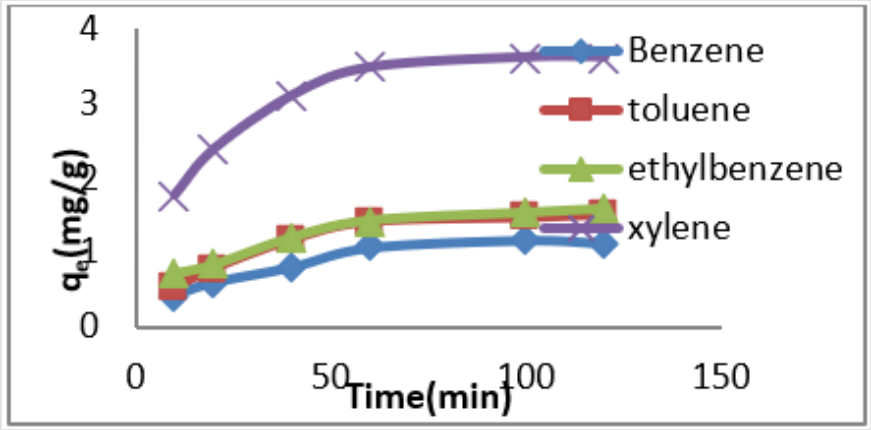

Figure 5: Effect of contact time on the removal of BTEX using Mt-HDTMA (BTEX solution = 50mg/L, initial pH= 7±0.5, contact time = 2hours, Mt-HDTMA = 0.5g).

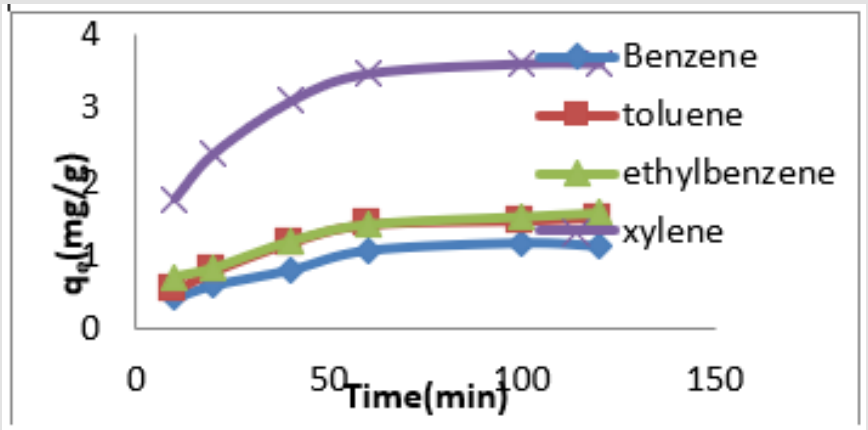

Figure 6: Effect of contact time on the adsorption of BTEX using Mt-TMPA (BTEX solution = 50mg/L, initial pH= 7±0.5, contact time = 2hours, Mt-TMPA =0.5g).

The order of the sorption capacities of the modified adsorbents are B <T <E <X. This order may be due to the water solubility [333,40,51], B (1790 mg/L) >T (530 mg/L) >E (152 mg/L) >X (150.5 mg/L) and the corresponding nature of hydrophobicity (based on log *k*ow) estimated as B = 2.13, T = 2.69, E = 3.15, and X = 3.15 [61]. Many previous studies have confirmed that the sorption of BTEX from aqueous solutions with various adsorbents (Table 3), follows a similar order as above [33,40,51,61,67]. Removal of BTEX by various adsorbents is presented in (Table 3). As seen, the adsorption capacity of BTEX with the modified clays in this study is high, especially for Ethylbenzene and Xylene. The removal efficiency of BTEX by TMPA-clay and Adam-clay, Bt-HDTMA and Bt-TMPA (Table 3). is nearly equal with values obtained for Mt-HDTMA, Mt-TMPA. However, the uptake efficiency for carbon nanotube (CNTNaOCl) and OMC-2NC were much higher than those of Mt-HDTMA, Mt-TMPA. Also, BTEX uptake efficiency by Mt-HDTMA, Mt-TMPA, were higher than those of Angico sawdust [51], peat [51], mature compost [68] and diatomite [61]. The effect of contact time on removing BTEX by raw Mt (Figure 4). showed that the adsorption capacity of the raw adsorbents for these compounds were about 7 to 10 times less than that for Mt-HDTMA, Mt-TMPA, Therefore, 2 hours was used as the optimum time for the other experiments.

Table 3: Comparison of BTEX removal of aqueous solution by adsorbent used in this study to those of other studies.

Adsorbent	B(mg/g)	T(mg/g)	E(mg/g)	X(mg/g)	Conditions	References
TMPA- clay	1.13	8.65	3.18	4.24		[25]
Adam-clay	0.47	4.32	1.59	2.41		[25]
Diatomite	0.031	0.037	0.042	0.042-0.09	5mg/L	[61]
CNT(NaOcl)	200	220	250	270	C0=100	[51]
Activated carbon	4.5	5	6	6.5	3 hours, 5mg/L	[61]
TTAB-clay	3.98	5.15	6	6.98	824hrs, 150mg/L	[33]
HDTMA-Kao	9.202	0.697	0.147	0.042	30min, 0.01mg/L	[79]
Angio-sawdast	0.00342	0.0041	0.00577	0.0107	C0=100	[51]
Peat	0.00341	0.0047	0.00581	0.019	C0=100	[51]
Mature Compost	1.12	1.59	2.16	3.5	C0=10mg/L,T=20 S/L=1/4g/L	[69]
Modified diatomite	0.0468	0.0552	0.0849	0.267	C0=5, S/ L=50/1g/L	[85]
OMN-2NC	12.7	32.9	37.7	58.7	C0=10, T=25 S/ L=1/4g/L	[86]
Bt-HDTM	1.53	1.58	1.69	3.74	2hrs, 50mg/L	[40]
Bt-TMPA	1.52	2	2.01	4.37	2hrs, 50mg/L	[40]
Mt-HDTM	1.228	1.462	2.132	4.618	2hrs, 50mg/L	This Study
Mt-TMPA	1724	1.506	2.58	4.618	2hrs, 50mg/L	This Study

Effect of Initial BTEX Concentration:

(Figures 7-9) shows the influences of initial BTEX concentrations between 50 and 200 mg/L on the sorption using montmorillonite (Mt), HDTMA modified montmorillonite (Mt-HDTMA), TMPA modified montmorillonite (Mt-TMPA) at initial pH of 7 ± 0.5 for 120 minutes. Based on the results, the initial concentration of BTEX has substantial role on the adsorption capacity. As seen, the adsorption capacities of the sorbents were increased by increasing BTEX concentration in the solution [69]. This may be due to an increase in driving forces affecting BTEX compounds. One of these forces is van der adsorbed at infinity. The plot of the fractional attainment to equilibrium (FATE) is shown in (Figures 10-12) for montmorillonite (Mt), HDTMA modified montmorillonite (Mt-HDTMA), TMPA modified montmorillonite (Mt-TMPA), 3.5.3. Intra-Particulate Diffusivity

The intraparticulate diffusivity was estimated using equation (2) which was developed using the linear driving force concept [70].

$$In[1-\alpha]=-kpt \quad (2)$$

where α is the fractional attainment to equilibrium (FATE) given by equation (3), Kp is the rate constant for intraparticulate diffusivity

$$\alpha=[m]-t/([M]) \quad (3)$$

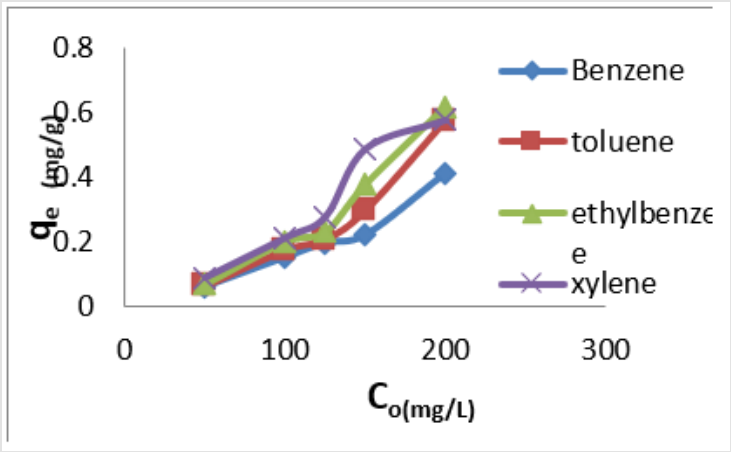

Figure 7: Effect of BTEX concentration on adsorption by Mt (Initial pH= 7± 0.5, contact time= 2 hours Mt conc = 5g/L).

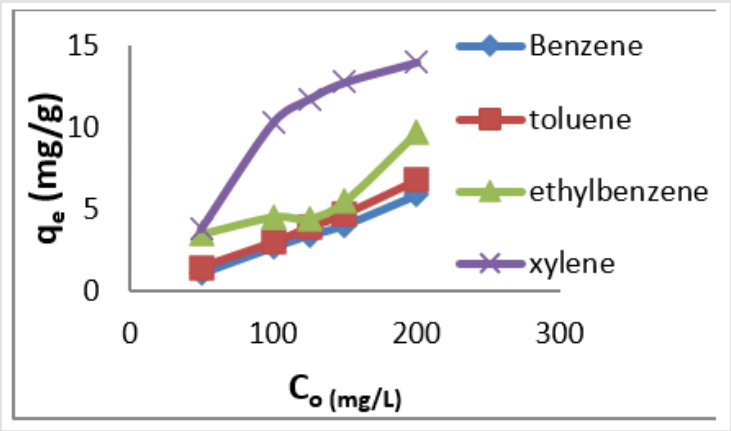

Figure 8: Effect of BTEX concentration on adsorption by Mt-HDTMA (Initial pH= 7± 0.5, contact time= 2 hours and Mt-HDTMA conc= 5g/L).

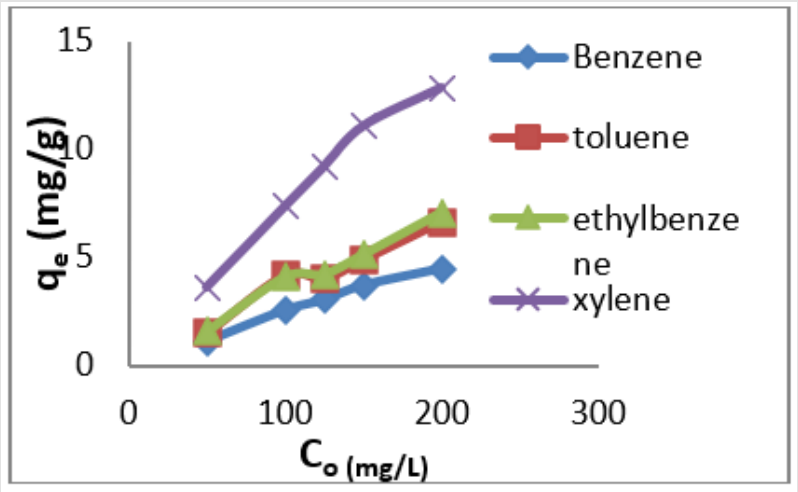

Figure 9: Effect of BTEX concentration on adsorption by Mt-TMPA (Initial pH= 7± 0.5, contact time= 2 hours and Mt-TMPA conc= 5g/L).

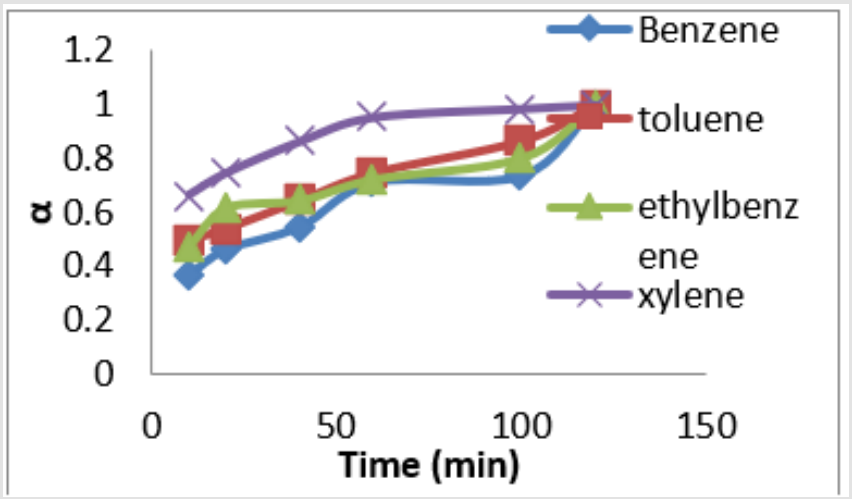

Figure 10: Fractional attainment to equilibrium (FATE) alpha against Time (min) for BTEX adsorption on Mt (BTEX conc = 50mg/L).

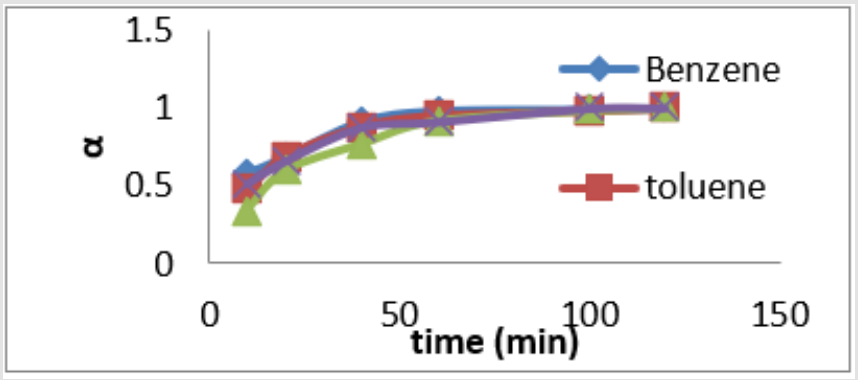

Figure 11: Fractional attainment to equilibrium (FATE) alpha against Time (min) for BTEX adsorption on Mt-HDTMA (BTEX conc = 50mg/L).

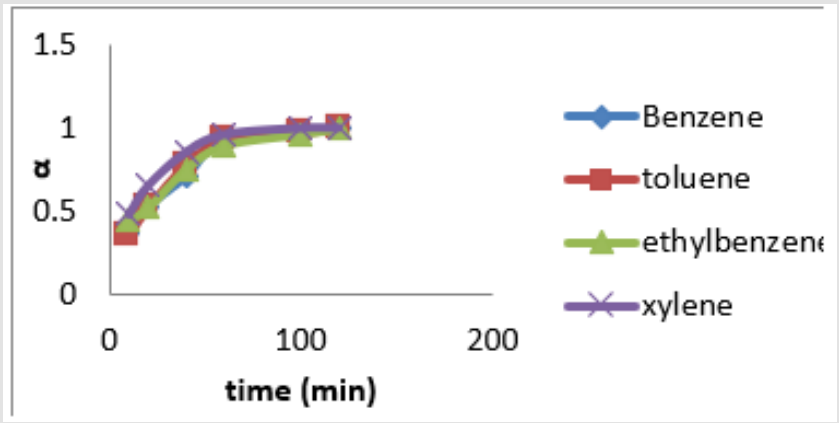

Figure 12: Fractional attainment to equilibrium (FATE) alpha against Time (min) for BTEX adsorption on Mt-TMPA (BTEX conc = 50mg/L).

where [M]t represents amount of BTEX adsorbed at time t and [M] the amount of BTEX 3.6. Adsorption Isotherm. Adsorption isotherm is one of the most important parameters to find the adsorption mechanism necessary for designing any sorption system [71]. It could be regarded as a graphical expression which described the amount or the quantity of the adsorbate that has been adsorbed onto the surface of the adsorbent at a particular operating condition [72]. Adsorption isotherms are precisely used to ascertain whether the adsorbent could be efficiently exploited for the removal of the adsorbate molecule from several solutions [73]. The use of adsorption isotherm model helps one to understand the process of adsorption [74]. The two widely used adsorption isotherm models include; Langmuir and Freundlich adsorption isotherm models. [33,74,75]. The Langmuir Isotherm model is a mathematical isotherm model, which is being obtained from theoretical approach or non experimental analysis and also has a constant referred to as Langmuir constant. The Langmuir isotherm model assumes that the adsorption of adsorbate molecule can only occur at a homogeneous site of the adsorbent and when this happen, no other adsorption will take place on the adsorbent surface [33, 73-75]. This isotherm model [40] in linear form is given as:

$$c\_\frac{e}{q}\_e = c\_\frac{e}{q}\_m + \frac{1}{(bq\_m)} \quad (4)$$

where Ce(mg/L) and qe(mg/g) are the concentration of adsorbate and the adsorption capacity of the adsorbent at the equilibrium time, respectively. b(L/mg) is the Langmuir constant and Qm(mg/g) is maximum adsorbent capacity. Qm and b are attained by the slope and intercept of Ce/qe versus Ce, respectively. The values of the Langmuir isotherm parameters are shown in (Table 4a). Lngmuir isotherm rather fitted poorly to the experimental data. Similar result was obtained by Nourmoradi et al. [33]; Onwuka et al [40].

Freundlich isotherm model is an empirical adsorption isotherm model which explains the equilibrium relationships existing between the adsorbate and the adsorbent molecules and assumes multi layer adsorption on the adsorbent heterogeneous site. The Freundlich isotherm model [73,75,76] is given as;

$$Inq\_e = Ink\_\frac{f+1}{nInC\_e} \quad (5)$$

qe and Ce are the adsorption capacity (mg/g) and the concentration (mg/L) of the adsorbate at equilibrium. The values of 1/n and kf are gotten from the linear plot of Inqe against In Ce. 1/n is the slope of the graph while kf is the intercept on y-axis, which are the Freundlich constant relating to heterogeneity of the adsorbent surface and adsorption capacity respectively [75]. The Freundlich isotherm parameters and its correlation coefficient (R^2) for BTEX adsorption by Mt-HDTMA and Mt-TMPA are exhibited in (Table 4a). The results show that Freundlich isotherm model fits well to the experimental data. Many researchers have shown that sorption of BTEX from aqueous solutions with different adsorbents is described well by Freundlich isotherm model [23,26,33,40,51,61]. The adsorption bond between adsorbent and adsorbate would be relatively strong if the $n$value, obtained from Freundlich isotherm model, is greater than one [76].

Table 4a: Parameter for Halsey, Lanmuir and Freundlich isotherms for the adsorption of BTEX.

Adsorbent	Adsorbate	Halsey				Langmuir		Freundlich		
		K_H	N_H	R^2	$Q_{m(mg/g)}$	B(L/mg/g)	R^2	$K_{f(mg/g)}$	n	R^2
Mt	Benzene	0.0152	0.7	0.994	-0.513	0.0116	0.812	0.0033	0.733	0.979
	Toulene	0.0128	0.75	0.989	-0.352	0.0116	0.945	0.156	4.695	0.11
	Ethylbenzene	0.0191	0.633	0.983	-1.126	0.0058	0.88	0.618	2703	0.002
	Xylene	0.0811	1.992	0.065	-0.347	0.0065	0.021	0.011	1184	0.111
Mt-HDTM	Benzene	0.0272	0.669	0.992	-4.926	0.0676	0.987	69.893	0.657	0.992
	Toulene	0.504	0.679	0.99	-6.579	0.736	0.965	9.459	0.679	0.99
	Ethylbenzene	2.563	0.548	0.009	-6.879	0.255	0.902	1.218	2.105	0.996
	Xylene	4.727	0.883	0.457	-11.494	0.0237	0.888	1.406	0.611	0.992
Mt-TMPA	Benzene	0.246	0.783	0.998	-10.101	0.0237	0.985	0.166	0.781	0.998
	Toulene	0.523	0.6358	0.833	6.494	0.0764	0.685	0.407	0.682	0.994
	Ethylbenz	0.68	0.617	0.727	5.076	0.1170	0.899	0.514	0.64	0.989
	Xylene	1.401	0.767	0.988	32.258	0.0143	0.814	1.77	0.797	0.997

Therefore, the $n$values of 2.61 to 1.66 for Mt-HDTMA and 3.80 to 1.78 for Mt-TMPA obtained by this isotherm model showed that BTEX is suitably adsorbed by Mt-HDTMA, Mt-TMPA, compared to Mt whose values are inconsistent with some values less than 1, indicating weak adsorption bonds between adsorbents and adsorbates. Nourmoradi et al [33] and Sharmasarkar et al [25]. reported that the n values for the removal of BTEX via the cationic modified clays (TTAB-Mt) and (TMPA-SWy and Adam-SWy) were

in range of 1.04 to 1.55 and 1.59 to 1.88 respectively . The Dubinin-Radushkevich isotherm (*D-R*) model has been used to determine the type of adsorption process as physical, chemical adsorption or ion exchange [33,77]. The linear form of the *D-R*isotherm model can be shown as:

$$Inq_e = Inq_m - \beta\varepsilon^2 \quad (6)$$

where, *qm*(mg/g) is the theoretical sorption capacity based on the isotherm, β(kJ/mol) is related to mean adsorption energy and ε (Polanyi Potential) is equal to *R*T ln (1 + 1/Ce). *R*(kJ/mol-K) is the universal gas constant and (K) is temperature [77]. From (Figures 13, 14 & 15) *qm* and β are obtained from the intercept and slope ln *qe*versus ε2, respectively. *E*(kJ/mol) is the mean adsorption energy that is illustrated by equation (7):

$$E = \frac{1}{(\sqrt{2\beta})} \quad (7)$$

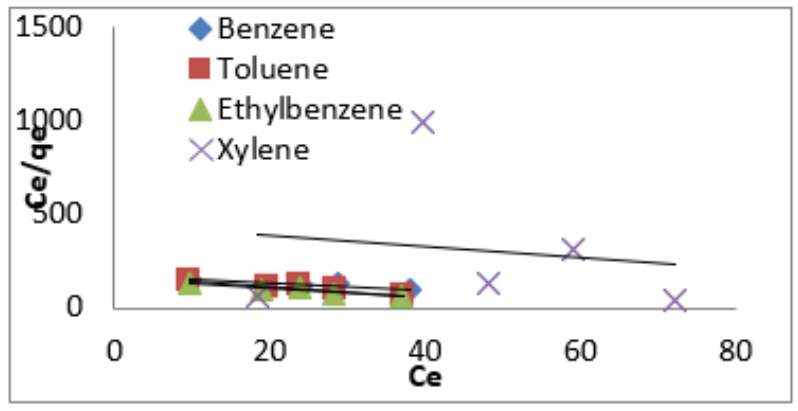

Figure 13: Langmuir Isotherm model for the adsorption of BTEX by Mt.

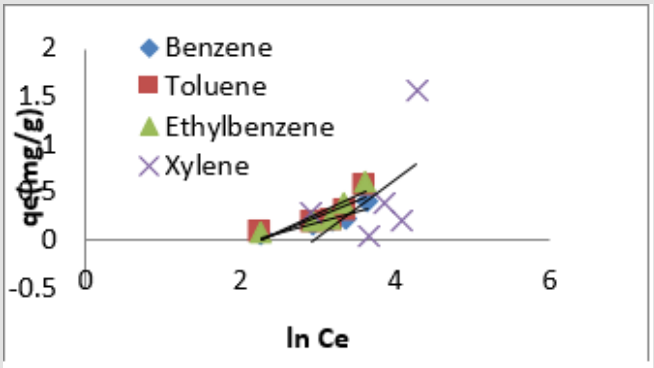

Figure 14: Temkin Isotherm model for the adsorption of BTEX by Mt.

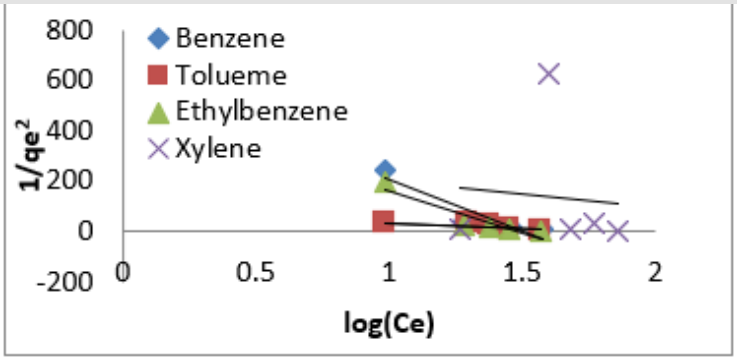

Figure 15: Harkins-Jara Isotherm model for the adsorption of BTEX by Mt.

The type of adsorption process is specified by the *E*value as follow: The physical and chemical adsorptions occurs if E < 8 kJ/mol or E > 16 kJ/mol, respectively. But the chemical ion exchange occurs for *E*in the 8–16 kJ/mol [78]. The values of parameters for *D-R* isotherm model for adsorption of BTEX by Mt, Mt-HDTMA, Mt-TMPA, are presented in (Table 4b). As seen, the adsorption of BTEX through Mt, Mt-HDTMA and Mt-TMPA, has occurred for *E*values in the range of 0.023 -0.11, 0.041-0.12, 0.028-0.057 kJ/mol for Mt, Mt-HDTMA and Mt-TMPA, respectively. Hence, the removal of BTEX in the solution by Mt, Mt-HDTMA and Mt-TMPA is governed by the physical adsorption.

Table 4b: Parameter for Temkin,Dubin Radushkevick and Harkins- jara isoterms for the adsorption of BTEX.

Adsorbent	Adsorbate	Temkin				Dubin Radushkevick		Harkins-jara		
		A(L/mg)	b	R^2	$q_{m(mg/g)}$	E(kj/mol)	R^2	A_H	B_H	R^2
Mt	Benzene	0.953	1.203	0.818	0.303	0.0127	0.844	0.0024	1.49	0.866
	Toulene	0.907	7.64	0.759	0.302	0.841	0.874	0.0024	1.78	0.631
	Ethylbenzene	0.883	6.644	0.81	0.912	0.0116	0.256	0.0029	1.45	0.853
	Xylene	0.673	4.469	0.257	0	0.016	0.886	0.0089	2.82	0.008
Mt-HDTM	Benzene	0.0007	0.632	0.879	3.963	0.016	0.808	0.563	101	0.918
	Toulene	0.0007	0.518	0.89	6.924	0.0405	0.92	0.959	0.84	0.904
	Ethylbenzene	0.0382	-2.02	0.051	6.062	0.116	0.978	38.46	2.08	0.039
	Xylene	2.602	0.331	0.358	22.065	0.0848	0.996	6.623	0.32	0.56
Mt-TMPA	Benzene	0.019	0.864	0.947	4.768	0.0276	0.857	0.596	1.09	0.93
	Toulene	0.0065	0.534	0.702	6.952	0.0456	0.742	0.825	0.75	0.979
	Ethylbenzene	0.065	0.527	0.5	8.085	0.0511	0.686	0.838	0.63	0.906
	Xylene	0.00005	0.273	0.901	15.287	0.0566	0.949	5.78	0.69	0.939

The Temkin model takes into account the effects of indirect adsorbate-adsorbate interactions on the adsorption isotherm and the heat of adsorption tends to decrease with increasing coverage due to these interactions [35,79]. The derivation of the Temkin model is based on the assumption that the decrease of the heat of adsorption with temperature is linear rather than logarithmic as implied by the Freundlich equation. The linear form of the Temkin model is given by Eq. (8).

$$q\_e = \frac{RT}{b} InA + \frac{RT}{bInC\_e} \quad (8)$$

where A (L.mg-1) and b are Temkin isotherm constants, R = 0.0083kJmol-1 K-1 and T is temperature (K) of the experiment. A plot of *qe* versus *InCe* is linear and the Temkin constants determined from the slope and intercept. From (Figures 16,17 & 18) it can be seen that the Temkin isotherm fitted rather poorly to the experimental data. Similar result was also obtained by Egbuchunam et al [79]. Halsey isotherm describes condensation of a multilayer at a relatively large distance from the surface [80]. This equations are suitable for multilayer adsorption and the poor fitting of the experimental data to this equation attest to the non-heteroporous nature of Mt, Mt-HDTMA and Mt-TMPA [81].The Linear form of this equation is given as follow:

$$\log e = \frac{1}{nH} \log k \frac{H-1}{n\_H} \log C\_e \quad (9)$$

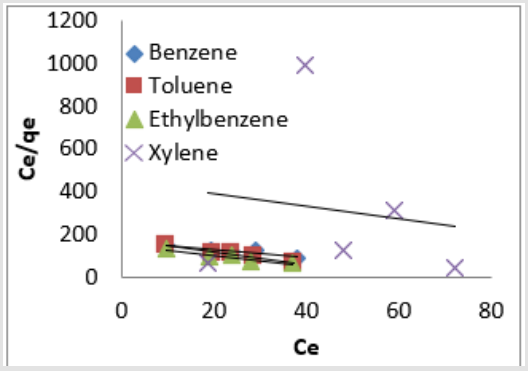

Figure 16: Langmuir Isotherm model for the adsorption of BTEX by Mt.

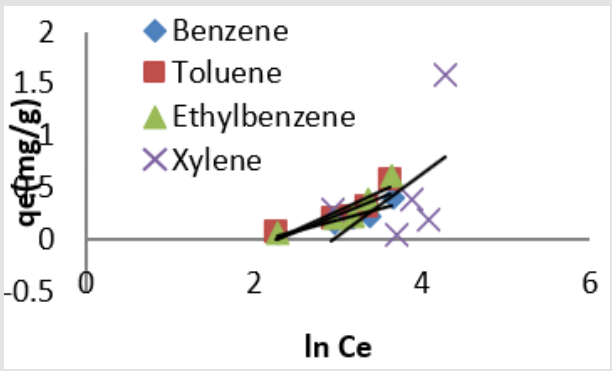

Figure 17: Temkin Isotherm model for the adsorption of BTEX by Mt.

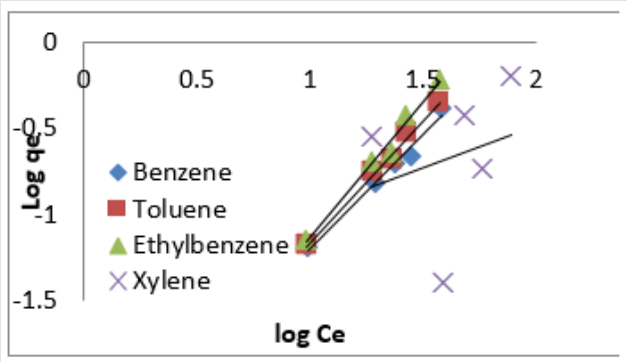

Figure 18: Harkins-Jara Isotherm model for the adsorption of BTEX by Mt.

The Halsey isotherm parameters are obtained from the plot of logqe versus log Ce. Where nH and KH are isotherm constants. (Figures 19, 20 & 21) shows linear Halsey isotherms graph. The constants and correlation coefficients of the related equation are listed in (Table 4a). The fitting of the Halsey isotherm equation was very low R^2 =0 in some cases, suggesting non-heteroporosity of the adsorbents [82].

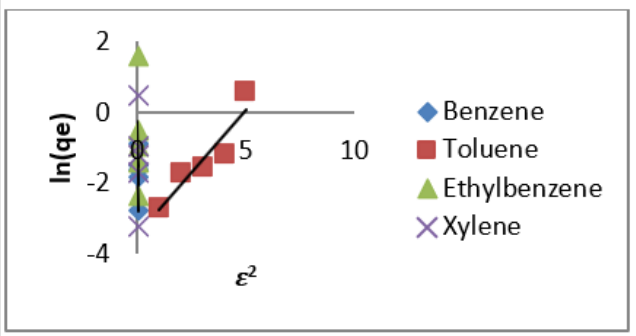

Figure 19: Dubnin-Radushkevich Isotherm model for the adsorption of BTEX by Mt.

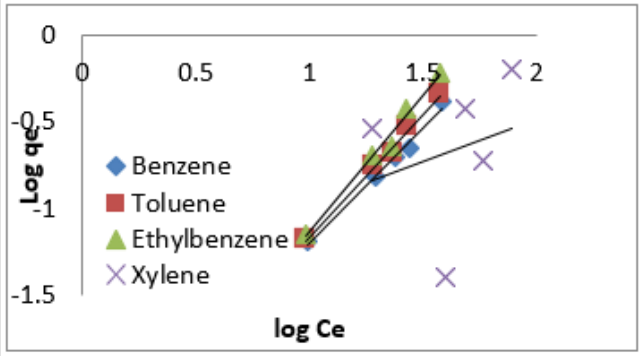

Figure 20: Halsey Isotherm model for the adsorption of BTEX by Mt.

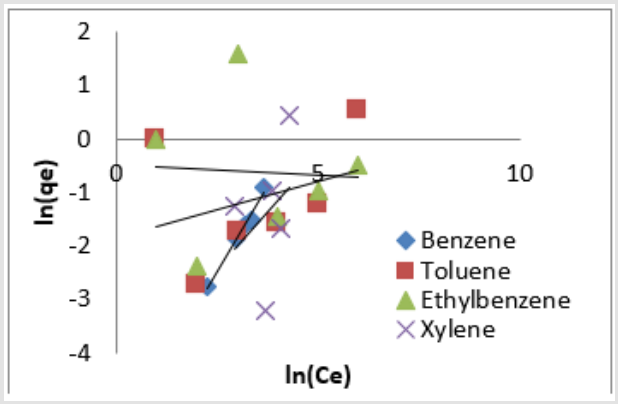

Figure 21: Freundlich Isotherm model for the adsorption of BTEX by Mt.

The Harkins-Jura adsorption isotherm accounts to multilayer adsorption and can be explained with the existence of heterogeneous pore distribution. The linear form of Harkins-Jura adsorption isotherm can be expressed as

$$\frac{1}{q_e^2} = \frac{B_{HJ}}{A_{HJ}} - \frac{LogC_e}{A_{HJ}} \quad (10)$$

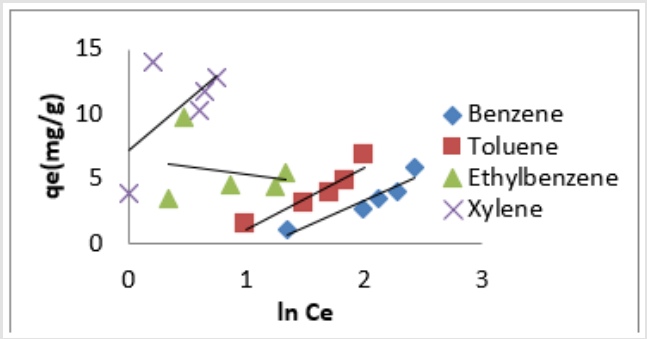

Figure 22: Temkin Isotherm model for the adsorption of BTEX by Mt-HDTMA.

AHJ is Harkins-Jura isotherm parameter which accounts for multilayer adsorption and explains the existence of heterogeneous pore distribution, BHJ is the isotherm constants (Ali et al., 2017). The Harkins-Jura isotherm models for BTEX adsorption onto Mt, Mt-HDTMA and Mt-TMPA are presented in (Figures 22, 23, 24) and the relevant isotherm parameters (Table 4b) shows that the low values of R^2 reveals the unlikelihood of the existence of heterogeneous pore distribution in Mt, Mt-HDTMA and Mt-TMPA. 3.6.1 Statistical Validation of Isotherm Model Percentage (%) residual error analysis was carried out to determine the best fitness, suitability and agreement of isotherm models and this was done using normalized standard deviation Δq (%) of root mean square residual error to compare the validity of each of the isotherm models more efficiently [83]. This is according to the relation.

$$\Delta q(\%) = 100 \times \sqrt{(\Sigma[q_e^{exp} - q_e^{cal} / q_e^{exp}]^2 / (n-1)} \quad (11)$$

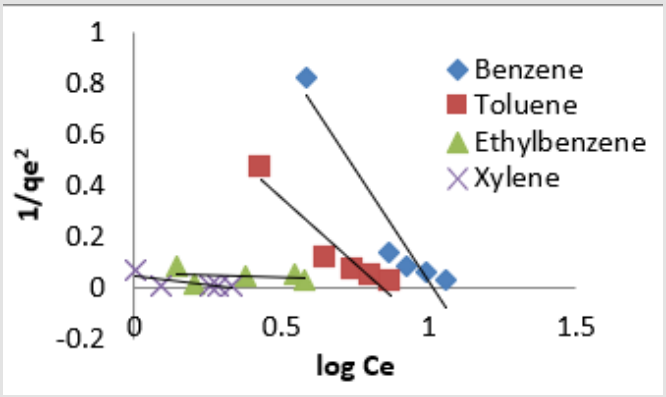

Figure 23: Harkins-Jara Isotherm model for the adsorption of BTEX by Mt-HDTMA.

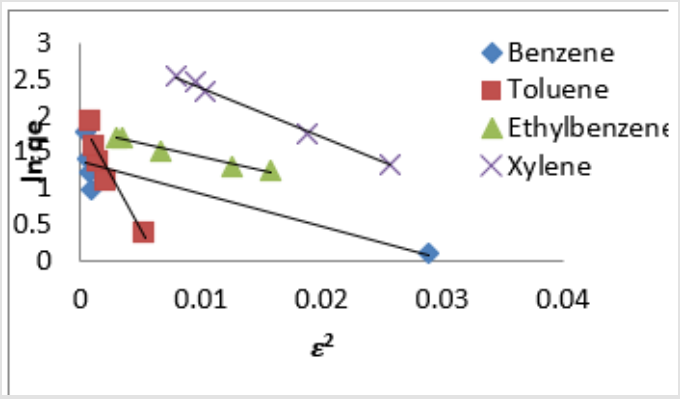

Figure 24: Dubnin-Radushkevich Isotherm model for the adsorption of BTEX by Mt-HDTMA.

The qeexpand qecal are the experimental and calculated values respectively and n is the number of measurements. The values of Δq are also given in (Table 5). It can been seen that the lowest values obtained for benzene, toluene, ethylbenzene and xylene for modified clays were in the range of Δq=2.19% to Δq=9.69% for Freundlich isotherm, and the highest value 102.98% was obtained for ethylbenzene for Langmuir isotherm (for Mt).Therefore, the Freundlich isotherm model was considered to describe the satisfactory fit with the sorption process since the value of Δq(%) is less than <10% [40]. Similar results was obtained by 40,82,83].

Table 5: Percentage Δqe values for Adsorption Isotherms.

Adsorbent	Adsorbate	Langmuir	Temkin	Halsey	Freundlich	Harkins-Jara	DubninRadushkevich
Mt	Benzene	Δq=76.34%	Δq=56.876%	Δq=19.76%	Δq=19.65%	Δq=91.98%	Δq=65.89%
	Toulene	Δq=65.63%	Δq=87.654%	Δq=29.86%	Δq=17.507%	Δq=77.008%	Δq=18.543%
	Ethylbenz	Δq=102.98%	Δq=54.287%	Δq=94.65%	Δq=14.599%	Δq=78.41%	Δq=90.56%
	Xylene	Δq=65.89%	Δq=76.76%	Δq=65.45%	Δq=13.876%	Δq=65.98%	Δq=45.7%
Mt-HDTMA	Benzene	Δq=49.76%	Δq=65.987%	Δq=55.9%	Δq=5.87%	Δq=52.981%	Δq=69.651%
	Toulene	Δq=54.98%	Δq=93.287%	Δq=19.64%	Δq=5.31%	Δq=87.542%	Δq=91.26%
	Ethylbenzene	Δq=78.84%	Δq=34.54%	Δq=35.69%	Δq=9.1%	Δq=75.776%	Δq=87.35%
	Xylene	Δq=87.65%	Δq=76.98%	Δq=45.876%	Δq=2.19%	Δq=29.31%	Δq=86.21%
Mt-TMPA	Benzene	Δq=65.73%	Δq=46.9%	Δq=61.45%	Δq=2.309%	Δq=98.54%	Δq=65.778%
	Toulene	Δq=48.901%	Δq=74.621%	Δq=35.95%	Δq=9.69%	Δq=57.811%	Δq=43.432%
	Ethylbenzene	Δq=48.677%	Δq=43.85%	Δq=59.31%	Δq=3.879%	Δq=54.81%	Δq=84.989%
	Xylene	Δq=54.321%	Δq=45.551%	Δq=54.987%	Δq=4.549%	Δq=96.23%	Δq=43.87%

Adsorption Kinetics

Adsorption kinetics is one of the most important parameters for determining the adsorption mechanism and also to investigate the efficacy of adsorbent for the removal of pollutants [33]. In this study, three kinetic models; pseudo-first-order, pseudo-second-order, and intra-particle diffusion models, were used to predict the sorption behavior of the data (Figures 25-38). below, represents various plots for these adsorption kinetic models. The pseudo-first-order kinetic model known as the Lagergren equation [49] is defined as

$$\log(q_e - q_t) = \log q_e - (\frac{k_1}{2.303})t \quad (12)$$

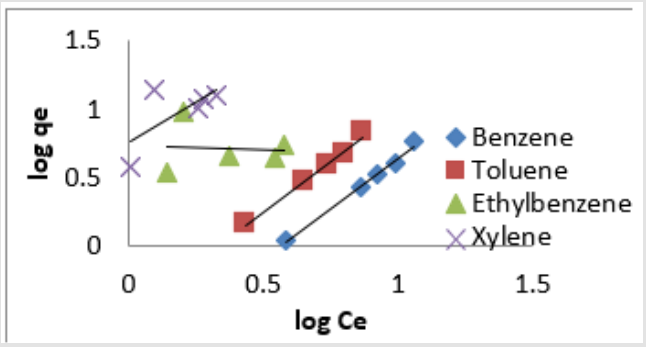

Figure 25: Halsey Isotherm model for the adsorption of BTEX by Mt-HDTMA.

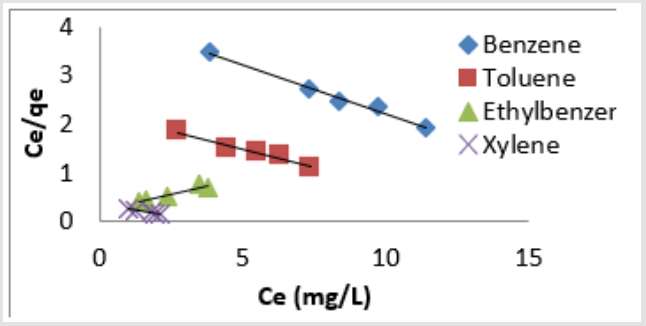

Figure 26: Langmuir Isotherm model for the adsorption of BTEX by Mt-HDTMA.

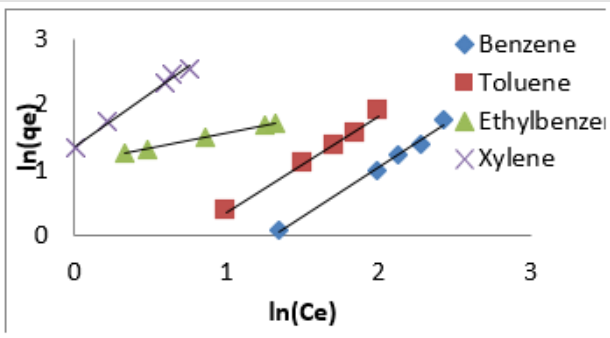

Figure 27: Freundlich Isotherm model for the adsorption of BTEX by Mt-HDTMA.

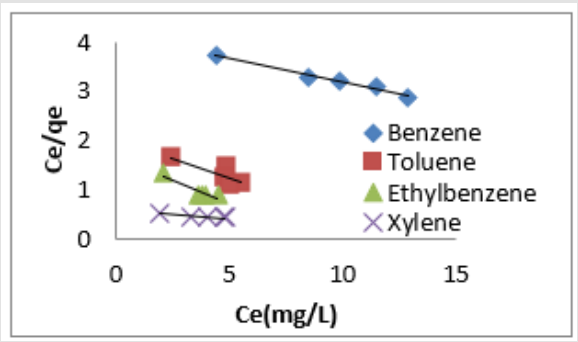

Figure 28: Langmuir Isotherm model for the adsorption of BTEX by Mt-TMPA.

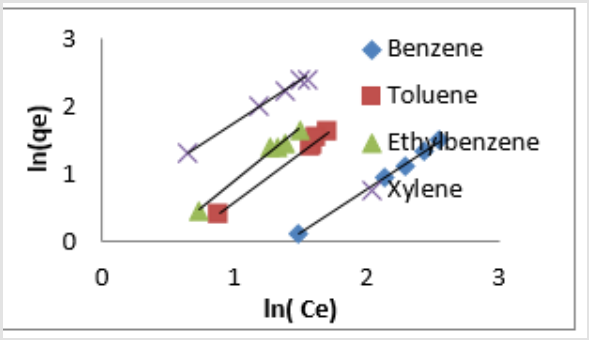

Figure 29: Freundlich Isotherm model for the adsorption of BTEX by Mt-TMPA.

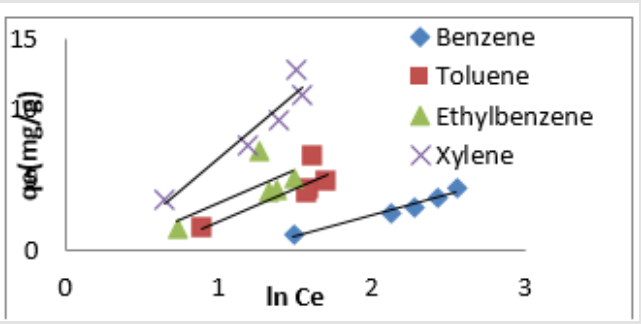

Figure 30: Temkin Isotherm model for the adsorption of BTEX by Mt-TMPA.

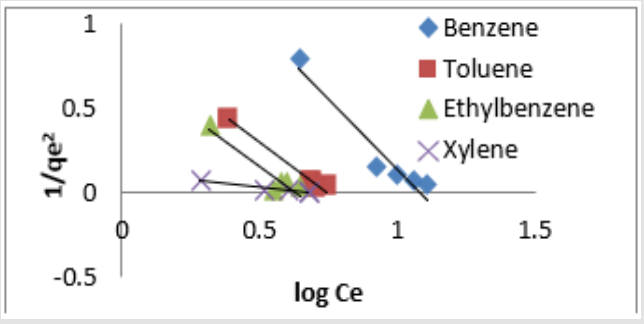

Figure 31: Harkins-Jara Isotherm model for the adsorption of BTEX by Mt-TMPA.

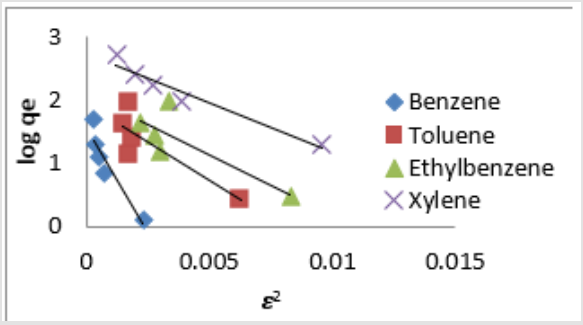

Figure 32: Dubnin Radushkevich Isotherm model for the adsorption of BTEX by Mt-TMPA.

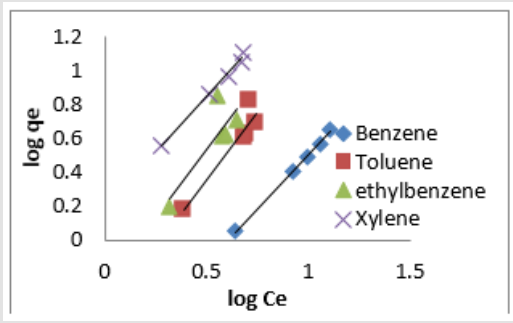

Figure 33: Halsey Isotherm model for the adsorption of BTEX by Mt-TMPA.

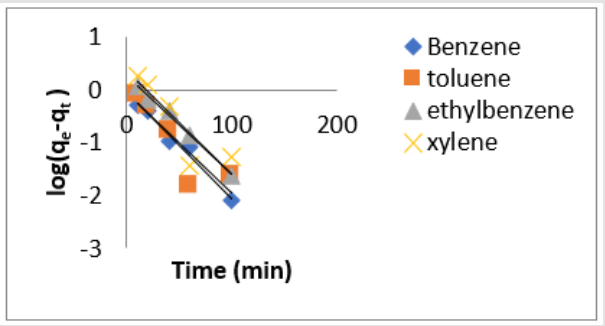

Figure 34: Pseudo Second Order model for the adsorption of BTEX by Mt.

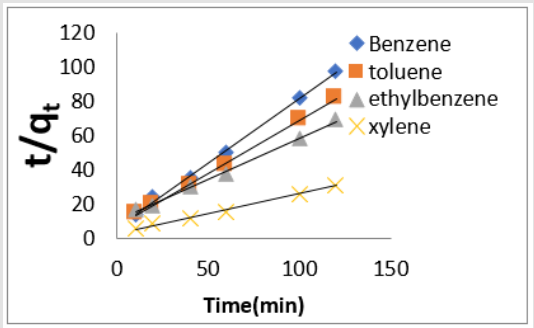

Figure 35: Intra-particle Diffusion model for the adsorption of BTEX by Mt.

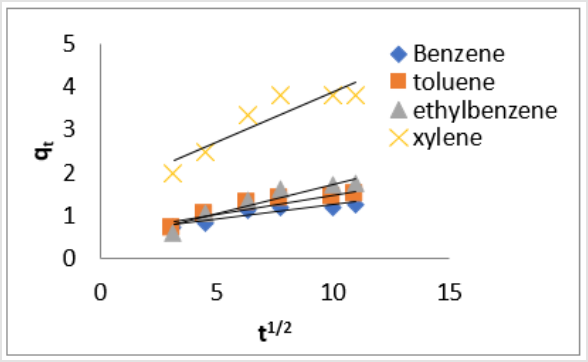

Figure 36: Pseudo First Order model for the adsorption of BTEX by Mt-HDTMA.

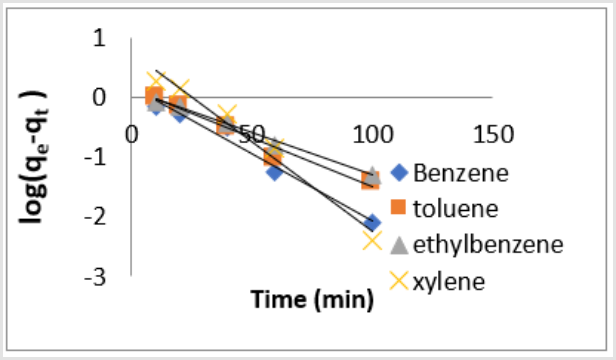

Figure 37: Pseudo Second Order model for the adsorption of BTEX by Mt-HDTMA.

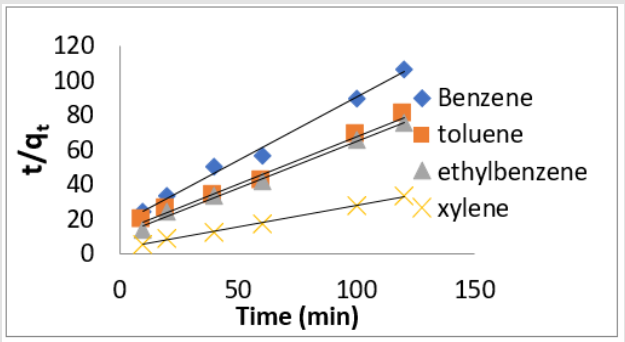

Figure 38: Intra-particle Diffusion model for the adsorption of BTEX by Mt-HDTMA.

where *qe* is the amount of BTEX adsorbed at equilibrium (mg/g), *qt* amount of BTEX adsorbed at any given time t (mg/g), k is the rate constant for the pseudo-first-order model. A plot of *lo*(*qe*− *qt*) against The pseudo-second-order model was also fitted to the adsorption data using the following equation [84]:

$$\frac{1}{q} = \frac{1}{k_2 q_e^2} + \frac{t}{q_e} \quad (13)$$

where qe and *qt* are the same as for the pseudo-first-order

parameters. $k2$ (g/mg-h) is the rate constant of pseudo-second order. In (Figure 39) $k2$ and qe values were obtained from the intercept and slope of linear plot of t/qt against t, respectively [33]. At initial stage of the adsorption process ($t \backsim 0$), the initial adsorption rate, h (g/mg -h), is obtained from;

$$h = k_2 q_e^2 \quad (14)$$

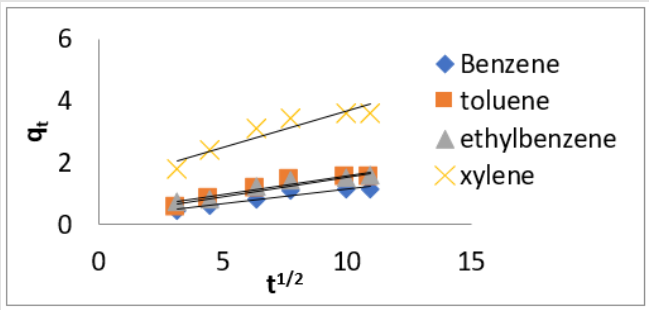

Figure 39: Pseudo First Order model for the adsorption of BTEX by Mt-TMPA.

The intra-particle diffusion kinetic model is mathematically described by the following equation [33]:

$$q_t = k_{id} t^{1/2} + c \quad (15)$$

where $k$id(g/mg-h) is the rate of the intraparticle diffusion kinetic model [51]. $k$idand $C$are obtained from the slope and intercept of qtversus $t1/2$, respectively.

(Figures 40 & 41) show plots of pseudo-second-order kinetic model for the adsorption of BTEX with Mt, Mt-HDTMA and Mt-TMPA. As can be seen from the correlation coefficient ($R2$), the pseudo-second-order kinetic model fits to the experimental data better than the other kinetic models (Figure 39). Moreover, the qe,calculated (mg/g) achieved using the pseudo-second-order kinetic model is rationally similar to the qe,experimental (mg/g) obtained from the experimental data. On the other hand, the pseudo-first-order and intra-particle diffusion models, because of the differences between calculated qe from the models and experimental qe, do not suitably predict BTEX sorption by the adsorbent. Aivalioti et al [61]. and Nourmoradi et al [33]. reported that sorption of BTEX with raw and thermally modified diatomite, and raw and TTAB modified montmorillonite respectively were described well by the pseudo-second-order kinetic model [33,61]. The parameters for pseudo-second- order kinetic model are listed in (Table 6) for Mt, Mt-HDTMA, Mt-TMPA. As seen, the values of the rate constant for pseudo-second-order kinetic models, $k2$(g/mg.h), follow the order of B >T >E >X, while the initial adsorption rate constant values of this kinetic model, h (g/mg - h), are shown to have the order of B <T <E <X.

Table 6a: Parameters of pseudo-first order, Pseudo Order Second, Intra Particle Diffusion Kinetic models Obtained from Mt Adsorption Data.

	Adsorbent Adsorbate	Mt Benzene	Toulene	Ethylbenzene	Xylene
Kinetic Model	Parameters				
Pseudo Order First	K_1	-0.004	-0.0009	-0.004	0.03
	q_e	0.384	0.576	0.333	0.147
	R^2	0.893	0.543	0.95	0.504
Pseudo Order Second	K^2	0.192	0.312	0.045	0.291
	$q_{e\ cal}$	0.182	0.148	0.319	0.465
	h	0.0064	0.0068	0.0076	0.083
	$q_{e\ exp}$	0.168	0.144	0.352	0.438
	R^2	0.919	0.969	0.308	0.998
Intra Particle Diffusion	K^{id}	0.011	0.008	0.008	0.019
	C	0.022	0.035	0.035	0.243
	R_2	0.916	0.977	0.977	0.929

Table 6b: Parameters of pseudo-first order, Pseudo Order Second, IntObtained from Mt-HDTMA Adsorption Data.

	Adsorbent Adsorbate	Mt Benzene	Toulene	Ethylbenzene	Xylene
Kinetic Model	Parameters				
Pseudo Order First	K_1	-0.019	-0.018	-0.018	-0.019
	q_e	0.936	0.928	1.291	1.441
	R^2	0.977	0.773	0.994	0.787

Pseudo Order Second	K^2	0.087	0.054	0.019	0.017
	$q_{e\ cal}$	1.329	1.616	2.283	4.219
	h	0.095	0.141	0.159	0.373
	$q_{e\ exp}$	1.228	1.462	2.132	4.5.04
	R2	0.998	0.998	0.997	0.996
Intra Particle Diffusion	K^{id}	0.065	0.091	0.138	0.235
	C	0.588	0.564	0.35	1.522
	R^2	0.83	0.833	0.897	0.846

Table 6c: Parameters of pseudo-first order, Pseudo Order Second, Intra Particle Diffusion Kinetic models Obtained from Mt-TPMA Adsorption Data.

	Adsorbent Adsorbate	Mt Benzene	Toulene	Ethylbenzene	Xylene
Kinetic Model	Parameters				
Pseudo Order First	K_1	-0.022	-0.016	-0.014	0.029
	q_e	1.198	1.149	1.125	2.102
	R^2	0.973	0.969	0.991	0.974
Pseudo Order Second	K^2	0.017	0.014	0.013	0.012
	$q_{e\ cal}$	1.823	2.384	2.64	4.292
	h	0.056	0.08	0.09	0.221
	$q_{e\ exp}$	1.724	1.506	2.584	4.618
	R^2	0.991	0.994	0.995	0.998
Intra Particle Diffusion	K^{id}	0.096	0.125	0.117	0.233
	C	0.176	0.254	0.376	1.331
	R_2	0.922	0.898	0.942	0.873

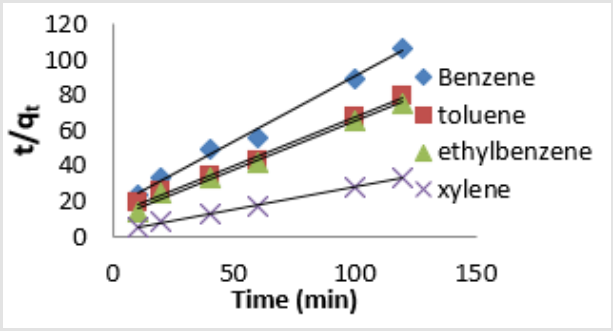

Figure 40: Pseudo First Order model for the adsorption of BTEX by Mt-TMPA.

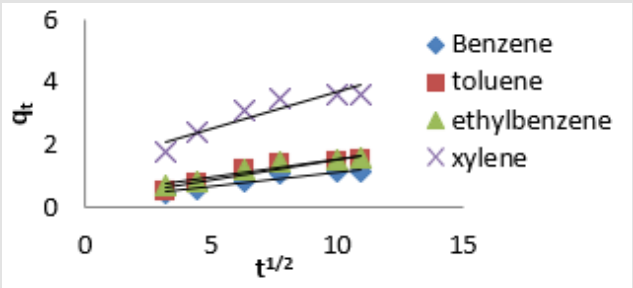

Figure 41: Intra-particle Diffusion model for the adsorption of BTEX by Mt-TMPA.

The reason for this (the order of h value) may be due to availability of more adsorption sites of the adsorbent at the beginning of the sorption process [33,67]. Hence, the lower hydrophilic compounds such as xylene and ethylbenzene have a higher tendency to the adsorbent, especially at the start of the adsorption process [85]. But as the time elapsed, the order of *k*2 value has a reverse relation with the order of h value. This may be attributed to the molecular weight of BTEX [86]. Due to lower molecular weight [33], benzene and then toluene can better penetrate onto the internal adsorption sites of the adsorbent as in comparison to higher-molecular weight compounds such as ethylbenzene and xylene.

Conclusion

Organophilicization of montmorillonite clay was achieved via intercalation mechanism involving the exchange of montmorillonite's surface cations with those of HDTMA and TMPA cationic surfactants. The modification enhanced the adsorption capacity of the new organoclay adsorbents for BTEX removal. The adsorption capacities of the synthesized organoclays for adsorption of BTEX was influenced by contact time and initial BTEX concentration. Freundlich isotherm and Pseudo second order kinetic models were best fits to sorption data. However, the adsorption capacities of the synthesized organoclays (Mt-HDTMA and Mt-TMPA) found to be 7-10 times greater than un-modified

montmorillonite (Mt) confirms that the synthesized organoclays are promising and suitable for hydrophobic sorption.

Conflict of Interest

Authors declare no conflict of interest.

Acknowledgement

Authors acknowledge the immense support of Gen. Umar S. Ikenwachukwu (Rtd).

References

1. Kansal A (2009) Sources and reactivity of NMHCs and VOCs in the atmosphere: a review. J Hazard Mater 166(1): 17-26.
2. Yurdakul S, Civan M, Tuncel G (2013) Volatile organic compounds in semi-urban Ankara atmosphere, Turkey: sources and variability. Atmos Res 120: 298-311.
3. Doherty BT, Kwok RK, Curry MD, Ekenga C, Chambers D, et al. (2017) Association between blood BTEXS concentrations and hematologic parameters among adult residents of the U.S Gulf States. Environ Res 156: 79-587.
4. Heibati B, Pollitt KJG, Karimi A, Yazdani Charati J, Ducatman A, et al. (2017) BTEX exposure assessment and quantitative risk assessment among petroleum product distributors. Ecotoxicol Environ Saf 144: 445-449.
5. Hosaini PN, Khan MF, Mustaffa NIH, Amil N, Mohamad N, et al. (2017) Concentration and source apportionment of volatile organic compounds (VOCs) in the ambient air of Kuala Lumpur, Malaysia. Nat Hazards 85(1): 437-452.
6. Afshari A, Schuch F, Marpu P (2018) Estimation of the traffic related anthropogenic heat release using BTEX measurements e a case study in Abu Dhabi. Urban Clim 24: 311-325.
7. Lee SC, Chiu MY, Ho KF, Zou SC, Wang X (2002) Volatile organic compounds (VOCs) in urban atmosphere of Hong Kong. Chemosphere 48(3): 375-382.
8. Buczynska AJ, Krata A, Stranger M, Locateli Godoi AF, Kontozova-Deutsch V, et al. (2009) Atmospheric BTEXconcentrations in an area with intensive street traffic. Atmos Environ43(2): 311-318.
9. Bolden AL, Kwiatkowski CF, ColbornT (2015) New look at BTEX: are ambient levels a problem. Environ. Sci Technol 49(9): 526-5276.
10. Latif MT, Hamid HHA, Ahamad F, Khan MF, Nadzir MSM, et al. (2019) BTEX compositions and its potential health impacts in Malaysia. Chemosphere 237: 124451.
11. Liu A, Hong N, Zhu P, Guan Y (2018) Understanding benzene series (BTEX) pollutant load characteristics in the urban environment. Sci Total Environ 619-620: 938-945.
12. Rattanajongjitrakorn P, Prueksasit T (2014) Temporal variation of BTEX at the area of petol station in Bangkok, Thailand. APCBEE Procedia 10: 37-41.
13. Moolla R, Curtis CJ, Knight J (2015) Occupational exposure of diesel station workers to BTEX compounds at a bus depot. Int J Environ Res Public Health 12(4): 4101-4115.
14. Tsangari X, Andrianou XD, Agapiou A, Mochalski P, Konstantinos C Makris (2017) Spatial characteristics of urinary BTEX concentrations in the general population. Chemosphere 173: 261-266.
15. Hildenbrand ZL, Mach PM, McBride EM, Dorreyatimm MN, Taylor JT, et al. (2016). Point source attribution of ambient contamination events near unconventional oil and gas development. Sci Total Environ 573: 382-388.
16. Jaggi A, Snowdon RW, Stopford A, Radovic JR, Oldenburg TBP, et al. (2017) Experimental simulation of crude oil-water partitioning behavior of BTEX compounds during a deep submarine oil spill. Org Geochem 108: 1-8.
17. Kumar A, Víden I (2007) Volatile organic compounds: sampling methods and their worldwide profile in ambient air. Environ Monit Assess 131(1-3): 301-21.
18. Bandura L, Kolodynska D, Franus W (2017) The Adsorption of BTX From Aqueous Solution By Na-PI Zeolite Obtained From Fly Ash process. saf environ prot 109: 214-223.
19. Tsakas MP, Siskos AP, Siskos P (2011) Indoor Air Pollutants and the Impact on Human Health. Chemistry, Emission Control, Radioactive Pollution and Indoor Air Quality, Nicolas Mazzeo Intech Open.
20. Ahmed Z, Doodhi H, Bhaumik A, Mazumdar S, Ray K (2019) The structural dynamics of the kinesin-2 stalk heterodimer and its biological relevance. Biochem Biophys Res Com, pp. 171-177.
21. Hoek G, Krishnan RM, Beelen R (2013) Long-term air pollution exposure and cardio- respiratory mortality: a review. Environ Health 12: 43.
22. Lara-Ibeas I, Megıas-Sayag C, Rodriguez-Cuevas A, Ocampo-Torres R (2020) Adsorbent Screening for Airborne BTEX Analysis And Removal. Journal of Environmental Chemical Engineering 8(2): 103563.
23. Lin SH, Huang CY (1999) Adsorption of BTEX from aqueous solution by macroreticular resins. J Hazard Mater 70: 21-37.
24. Zytner RG (1994) Sorption of benzene, toluene, ethylbenzeneand xylenes to various media. J Hazard Mater 38: 113-126.
25. Sharmasarkar S, Jaynes WF, Vance GF (2000) BTEX sorption by montmorillonite Organoclays: TMPA, ADAM, HDTMA. Water Air & Soil Pollut 119: 257-273.
26. Standeker S, Novak Z, Knez Z (2009) Removal of BTEX vapours from waste gas streams using silica aerogels of different hydrophobicity. J Hazard Mater165: 1114-1118.
27. Simpson JA, Bowman RS (2009) Nonequilibrium sorption andtransport of volatile petroleum hydrocarbons insurfactant-modified zeolite. J Contam Hydrol 108: 1-11.
28. Torabian A, Kazemian H, Seifi L, Bidhendi GN, Azimi AA, et al. (2010) Removal of petroleum aromatichydrocarbons by surfactant-modified natural zeolite: the effect of surfactant. CLEAN Soil Air Water 38: 77-83.
29. Aivalioti M, Vamvasakis I, Gidarakos E (2010) BTEX and MTB Eadsorption onto raw and thermally modified diatomite. J Hazard Mater 178: 136-143.
30. Moura CP, Vidal CB, Barros AL, Costa LS, Vasconellos LCG, et al. (2011) Adsorption of BTX (benzene, toluene, o-xylene, and p-xylene) from aqueoussolutions by modified periodic mesoporous organosilica. J Colloid Interface Sci. 363: 626-634.
31. Alejandro S, Valdés H, Manero MH, Zaror CA (2012) BTXabatement using Chilean natural zeolite: the role of Brønstedacid sites. Water Sci Technol 66: 1759-1765.
32. Simantiraki F, Aivalioti M, Gidarakos E (2012) Laboratory studyon the remediation of BTEX contaminated groundwater usingcompost and Greek natural zeolite. Crete Proceedings, p. 1-8.

33. Nourmoradi H, Nikaeen M, Khiadani M (2012) Multi-Component Adsorption of Benzene, Toluene, Ethylbenzene, and xylene from Aqueous solutions by Montmorillonite Modified with Tetradecyl Trimethyl Ammonium Bromide. journal of chemistry, p. 1-10.

34. Carvalho MN, Da Motta M, Benachour M, Sales DCS, Abreu CAM (2012) Evaluation of BTEX and phenol removal from aqueous solution by multi – solute adsorption onto smectite organoclay. J Hazard Mater, pp. 239-240, 95-101.

35. Vidal CB, Raulino GSC, Barros AL, Lima ACA, Ribeiro JP, et al. (2012) BTEX removal from aqueous solutions by HDTMA – modified Y zeolite. J Environ Manage 112: 178 -185.

36. Aleghafouri A, Hasanzadeh N, Mahdyarfar M, SeifKordi A, Mahdavi SM (2015) Experimental and theoreticalstudy on BTEX removal from aqueous solution of diethanolamine using activated carbon adsorption. J Nat Gas Sci Eng 22: 618-624.

37. Szala B, Bajda T, Matusik J, Zi eba K, Kijak B (2015) BTXsorption on Na-P1 organo-zeolite as a process controlled bythe amount of adsorbed HDTMA. Microporous Mesoporous Mater 202: 115-123.

38. Muir B, Bajda T (2016) Organically modified zeolites in petroleum compounds spill cleanup—production, efficiency, utilization. Fuel Process Technol 149: 153-162.

39. Bandura L, Panek R, Rotko M, Franus W (2016) Syntheticzeolites from fly ash for an effective trapping of BTX in gasstream. Microporous Mesoporous Mater 223: 1-9.

40. Onwuka KE, Igwe JC, Aghalibe CU, Obike AI (2020) Hexadecyltrimethyl Ammonium (HDTMA) and Trimethylphenyl Ammonium (TMPA) Cation's intercalation of Nigerian Bentonite Clay for Multi-component Adsorption of Benzene, Toluene, Ethylbenzene and Xylene (BTEX) From Aqueous Solution: Equilibrium and Kinetic Studies. Journal of Analytical Techniques and Research 2(2): 70-95.

41. Onwuka KE, Igwe JC, Enenwa NE, Aghalibe CU (2020) A Study of Pyrene Adsorption Behavior onto Oraganoclays in Aqueous Solution. International Journal of Prevention and Control of Industrial Pollution 6(2): 1-14.

42. Mortland MM, Shaobai S, Boyd SA (1986) Clay-organic complexes as adsorbents for phenol and chlorophenols. Clays Clay Miner 34: 581-585.

43. Koh SM, Dixon JB (2001) Preparation and application of organo-minerals as sorbents of phenol, benzene and toluene. Appl Clay Sci 18: 111-122.

44. Polabusova T, Rytwo G, Nir S, Serban C, Margulies L (1997) Adsorption of benzyltrimethyl ammonium and benzyltriethylammonium on montmorillonite; experimental studies and model calculations. Clays Clay Miner 45: 834-841.

45. Kooli F, Alshahateet SF (2008) Organomontmorillonites Having Different Charges for Wastewater Treatment: Adsorption of Phenol Molecules. J Int Environmental Application & Science 3(4): 207-214.

46. Shen Y (2002) Removal of phenol from water by adsorption-flocculation using organobentonite. Water Res 36: 1107-1114.

47. Baskaralingam P (2006) Equilibrium studies for the adsorption of acid dye onto modified hectorite. Journal of hazardous materials 136(3): 989-992.

48. Waanders EFF, Fourie CL (2015) Surfactant Impregnated Bentonite Clay for the Adsorption of Anionic Dye.7th International Conference on Latest Trends in Engineering & Technology (ICLTET'2015) Nov. 26-27, Irene, Pretoria (South Africa).

49. Trivedi HC, Patel VM, Patel RD (1973) Adsorption of cellulose triacetate on calcium silicate. European Polymer Journal 9(6): 525-531.

50. Doan M, Alkan M, Onganer Y (2000) Adsorption of methylene blue from aqueous solution onto perlite, Water Air and Soil Pollution 120(3-4): 229-248.

51. Su F, Lu C, Hu S (2010) Adsorption of benzene, toluene, ethylbenzene and p-xylene by NaOCl-oxidized carbon nanotubes. Colliod Surface A 353: 83-91.

52. Medejova J (2003) FTIR Technique of clay mineral studies. Vib Spectrosc 31: 1-10.

53. Putra EK, Pranowo R, Sunarso J, Indraswati N, Ismadji S (2009) Performance of activated carbon and bentonite for adsorption of amoxicillin from wastewater: Mechanisms, isotherms and kinetics. Water Res 43: 2419-2430.

54. Obi Chidi, Okike UN, Okoye P I (2018) The Use of Organophilic Bentonite in the Removal Phenol from Aqueous Solution: Effect of Preparation Techniques. Modern Chem Appl 6: 258.

55. Eren E, Afsin B (2008) An investigation of Cu (II) adsorption by raw and acid-activated bentonite: a combined potentiometric, thermodynamic, XRD, IR, DTA study. J Hazard Mater 151: 682-691.

56. Ikhtiyarova GA, Ozcan AS, Gok O, Ozcan A (2012) Characterization of natural-and organo- bentonite by XRD, SEM, FT-IR and thermal analysis techniques and its adsorption behaviour in aqueous solutions. Clay Minerals 47: 31-44.

57. Khenfi A, Bouberka Z, Sekrane F, Kameche M, Derriche Z (2007) Adsorption study of an industrial dye by an organic clay. Adsorption 13: 149-158.

58. Ozcan AS, Erdem B, Ozcan A (2004) Adsorption of acid blue 193 from aqueous solutions onto Na-bentonite and DTMA-bentonite. J Colloid Interface Sci 280: 44-54.

59. Cheol HD, Min HL, Young DK, Byoung HM, Jeong HK (2006) Effect of clay modifiers on the morphology and physical properties of thermoplastics polyurethane/clay nanocomposites. Polymer 47: 6718-6730.

60. Olugbenga AG, Garba MU, Soboyejo W, Chukwu G (2013) Beneficiation and characterization of a benetonite from Niger Delta region of Nigeria. Int J Sci Engg Invest 2: 14-18.

61. Aivalioti M, Vamvasakis L, Gidarakos E (2010) BTEX and MTBE adsorption onto raw and thermally modified diatomite. J Haz Mater 178(1–3): 136–143.

62. Kang DN, Jung KI, Kim SH, Jeon SH (2009) Computational-Aided Identification of Genes Regulated by the Drosophila Vnd. J Neurogenet 23(4): 355-365.

63. Tiwari M, Bajpai VK, Sahasrabuddhe AA, Kumar A, Sinha RA (2008) Inhibition of N-(4-hydroxyphenyl) retinamide-induced autophagy at a lower dose enhances cell death in malignant glioma cells. Carcinogenesis 29(3): 600-609.

64. Bankovic A, Makochekanwa C, Tattersall W, Peter AJ (2009) Total and positronium formation cross sections for positron scattering from H2O and HCOOH. New journal of physics 11(10): 103036.

65. Khenifi A, Zohra, B, Kahina B, Houari H, Zoubir D (2009) Removal of 2,4-DCP from wastewater by CTAB/bentonite using one-step and two-step methods: A comparative study. Chemical Engineering Journal 146: 345-354.

66. Carvalho MN, Da Motta M, Benachour M, Sales DCS, Abreu CAM (2012) Evaluation of BTEX and phenol removal from aqueous solution by multi – solute adsorption onto smectite organoclay. J Hazard Mater 239-240: 95-101.

67. Jiang QM, JinXY, Lu XQ, Chen ZL, (2010) Adsorption of Pb (II), Cd (II), Ni(II) and Cu(II) onto natural kaolinite clay, Desalination. 252 (1–3): 33-39.

68. Daifullah AAM, Girgis BS (2003) Impact of surface Characteristics of activated carbon on adsorption of BTEX. Colloids and Surfaces A 214(1–3): 181-193.

69. Bandura L, Panek R, Rotko M, Franus W (2016) Syntheticzeolites from fly ash for an effective trapping of BTX in gasstream. Microporous Mesoporous Mater 223: 1-9.

70. Okieimen FE, Okundia EU, Ogbeifun DE (1991) Sorption of cadmium and lead ions on modified groundnut (Arachis hypogea) husks. J Chem Technol Biotechnol 5(1): 97-103.

71. Igwe JC, Mbonu OF, Abia AA (2007) Sorption Kinetics, Intraparticle Diffusion and Equilibrium Partitioning of Azo Dyes on Great Millet (Andropogon Sorghum) Waste Biomass. J App Sci 7(19): 2840-2847.

72. Okpareke OC, Agha II, Ejikeme PM (2009) Removal of Cu (II), Cd (II) and Hg (II) ions from simulated waste water by Brachystagea Eurycoma seed pod: Intraparticle diffusivity and sorption studies, Paper presented at the 32nd. International Conference of the Chemical Society of Nigeria, Bauchi.

73. Eman AE (2013) Modified Activated Carbon and Benonite Used to Adsorb Petroleum Hydrocarbons Emulsified in Aqueous Solution. American Journal of Environmental Protection 2(6): 161-169.

74. Senturk BH, OzdesD, Gundogdu A, Duran C, Soylak M (2009) Removal Of Phenol From Aqueous Solutions By Adsorption Onto Organomodified Tirebolu Bentonite. Journal Of Harzardous Material 172: 353-362.

75. Ewuzie HE, Ekpo RE, Okeacha EG (2018) Multi Component Adsorption of Toluene, Ethyl Benzene and Meta- Xylene by Batch Adsorption Technique Using Natural and Acid Treated - Modified Sodium Bentonite. Int J Sci Res 8(2): 435-451.

76. Koyuncu H, Yildiz N, Salgın U, Köroğlu F, Çalimli A (2011) Adsorption of o-, m- and p-nitrophenols onto organically modified bentonites. J Haz Mater 185(2): 1332-1339.

77. Kul AR, Koyuncu H (2010) Adsorption of Pb(II) ions from aqueous solution by native and activated bentonite: kinetic, equilibrium and thermodynamic study. J Haz Mater 179(1–3): 332–339.

78. Cestari AR, Vieira EFS, Vieira GS, Almeida LE (2007) Aggregation and adsorption of reactive dyes in the presence of an anionic surfactant on mesoporous aminopropyl silica. Journal of Colloid and Interface Science. 309(2): 402-411.

79. Egbuchunam TO, Obi G, Okieimen FE, Tihminlioglu F (2016) Removal of BTEX from Aqueous Solution Using Organokaolinite. Int J App Environ Sci 11(2): 505-513.

80. Halsey G (1948) Physical adsorption on non-uniform surfaces. J Chem Phys16: 931-937.

81. Ali Q, Javed MT, Noman A, Haider MZ, Waseem M, et al. (2017) Assessment of drought tolerance in mung bean cultivars/lines as depicted by the activities of germination enzymes, seedling's antioxidative potential and nutrient acquisition. Arch Agron Soil Sci.

82. Ahmad MA, Alrozi R (2010) Optimization of Preparation Conditions for Mangosteen Peel-Based Activated Carbons For the Removal Of Remazol Brilliant Blue R Using Response Surface Methodology. Chemical Engineering Journal 165: 883-890

83. Oha TU (2017) Isotherm And Kinetic Studies Of Some Selected Dyes Adsorption From Aqueous Solution Using Palm Fruit Fibre. MSc Thesis Daepartment Of Pure And Industrial Chemistry Abia State University, Nigeria.

84. Ho YS, McKay G (1998) Sorption of Dye from Aqueous Solution by Peat. Chemical Engineering Journal 70(2): 115-124.

85. Makhathini TP, Rathilal S (2017) Investigation of BTEX compounds adsorption onto polystyrenic resin. South African Journal of Chemical Engineering 23: 71-80.

86. Lian Q, Konggidinata MI, Ahmad ZU, Gang DD, Yao L, et al. (2019) Combined effects of textural and surface properties of modified ordered mesoporous carbon (OMC) on BTEX adsorption. Journal of Hazardous Materials 377: 381-390.

ISSN: 2574-1241

DOI: 10.26717/BJSTR.2022.41.006678

Kelechi E Onwuka. Biomed J Sci & Tech Res